(Leu[17]δ$_1$,Phe[8]ε), (Leu[14]δ$_2$,Phe[8]ζ), (Val[3]γ,Leu[18]δ$_2$), (Phe[8]ε,Glu[13]γ), (Phe[8]δ,Glu[13]γ), (Ala[15]β,Tyr[1]ε), (Phe[8]α,Glu[13]β), (Tyr[1]δ,Ser[9]α), and (Phe[8]δ,Glu[13]β).

29. A simulated annealing (SA) protocol using NMRchitect (Biosym Technologies, San Diego, CA) was used to generate the ensemble of conformations consistent with the NMR data. The SA protocol was derived from that developed by M. Nilges, G. M. Clore, and A. M. Gronenborn [*FEBS Lett.* **239**, 129 (1988)] and was optimized for this system. Each NOE was classified as strong, medium, weak, or very weak on the basis of a linear fit of the measured volumes from NOESY spectra with mixing times of either 50, 100, and 200 ms (H_2O spectra) or 100 and 200 ms (D_2O spectra). The volumes were fit to a linear relation with mixing time and calibrated to volume measurements for cross peaks corresponding to known interproton distances. Most distance restraints were derived from NOE cross-peak volume measurements of NOESY spectra taken in H_2O. A few weak NOEs between side-chain protons were more readily analyzed from data collected in D_2O because of both the increased sensitivity of data collection and the reduced complexity of the spectra. Each NOE category was assigned a distance range: strong (1.0 to 2.5 Å), medium (1.8 to 3.5 Å), weak (1.8 to 5.0 Å), and very weak (1.8 to 5.5 Å). A maximum force constant of 25 kcal mol^{-1} Å^{-2} was used for all NOE distance restraints. Pseudoatoms were used when necessary, and standard corrections were applied to interproton distances involving pseudoatoms (*35*). The use of pseudoatoms resulted in the generation of 301 restraints from 367 NOE volume measurements. An alternate conformation accounting for less than 15% of the total signal was visible in the NMR spectra and assigned through NOE analysis to the cis conformation of DPro[4]. Cross peaks from the NOESY attributable to this conformation were omitted for the generation of restraints. Dihedral restraints were included in the SA analysis to enforce trans geometry of the amide bond between Val[3] and DPro[4].
30. The C-terminal glycine was poorly defined by the NMR data and was therefore excluded from the RMSD calculation to yield values of 0.90 Å for backbone atoms and 1.37 Å for the heavy atoms of residues 1 through 22. When Gly[23] was included in this calculation, the RMSD of the coordinates for all residues from the average structure was 1.28 Å for backbone atoms and 1.51 Å for all heavy atoms.
31. M. S. Lee, G. P. Gippert, K. V. Soman, D. A. Case, P. E. Wright, *Science* **245**, 635 (1989).
32. G. V. Semisotnov *et al.*, *Biopolymers* **31**, 119 (1991).
33. The presence of discrete tertiary structure is often probed by studying the interaction of this hydrophobic, fluorescent dye with proteins. Although ANS will bind to the apolar regions of partially folded or "molten globule" states of proteins, native folded proteins do not bind ANS. Many designed proteins to date have demonstrated significant ANS binding, which is attributed to poor tertiary packing interaction and the adoption of "molten globule" rather than native-like states (*7, 11*). BBA1 did not enhance the fluorescence of ANS, indicating that this designed peptide does not bind ANS under conditions (*5*) previously shown to establish the presence of these poorly folded states. Experiments were performed in 20 mM acetate buffer, pH 4.5, and 30 μM BBA1 with ANS concentrations ranging from 20 to 600 μM. The results indicate that the apolar side chains of BBA1 are sufficiently buried in the folded structure to preclude interaction with the dye.
34. D. B. Wetlaufer, *Trends Biochem. Sci.* **15**, 414 (1990).
35. K. Wüthrich, *NMR of Proteins and Nucleic Acids* (Wiley, New York, 1986).
36. This work was supported by NSF grant CHE-910445, a Parsons Foundation predoctoral fellowship (M.D.S.), an NIH traineeship (R.P.C.), and a Camille and Henry Dreyfus Teacher Scholar Award (B.I.). We gratefully acknowledge the Dorothy Chandler, Camilla Chandler Frost Laboratory in Biology at the California Institute of Technology for use of the Varian Unity Plus 600 NMR Spectrometer.

17 August 1995; accepted 13 November 1995

Assembly of a Ribonucleoprotein Catalyst by Tertiary Structure Capture

Kevin M. Weeks and Thomas R. Cech

CBP2 is an RNA tertiary structure binding protein required for efficient splicing of a yeast mitochondrial group I intron. CBP2 must wait for folding of the two RNA domains that make up the catalytic core before it can bind. In a subsequent step, association of the 5′ domain of the RNA is stabilized by additional interactions with the protein. Thus, CBP2 functions primarily to capture otherwise transient RNA tertiary structures. This simple one-RNA, one-protein system has revealed how the kinetic pathway of RNA folding can direct the assembly of a specific ribonucleoprotein complex. There are parallels to steps in the formation of a much more complex ribonucleoprotein, the 30S ribosomal subunit.

Several processes essential for gene expression are carried out by ancient machinery whose function requires the interplay of RNA and protein components. These ribonucleoprotein (RNP) enzymes include ribonuclease P, the spliceosome, and the ribosome (*1*). Although much is known about the order of assembly of complex RNPs from their RNA and protein components, the kinetic pathways of assembly are poorly understood.

Excision of the group I intron bI5, the fifth intron in the cytochrome b pre–messenger RNA in yeast mitochondria, is carried out by a simple RNP composed of the RNA intron and the splicing factor CBP2 (*2*). The intron RNA consists of three domains of ~100 nt each (Fig. 1A) (*3*). Under near-physiological Mg^{2+} concentrations (7 mM), the RNA is in a state (termed 2°) in which the secondary structure is formed but higher order structure is largely absent. Studies of the RNA at equilibrium (*3, 4*) have revealed a pathway for formation of the active tertiary structure in the absence of CBP2. First, the P5-P4-P6 and P7-P3-P8 domains associate to form the catalytic core (termed the core state). The 5′ domain, which includes P1, the site of guanosine addition in the first step of splicing, then associates with the core to form the active, assembled ribozyme (E):

$$\text{RNA } 2° \rightleftarrows \text{core} \rightleftarrows \text{E} \qquad (1)$$

Mg^{2+} promotes formation of the core state in a cooperative transition that is complete at 40 mM divalent ion; however, Mg^{2+} does not efficiently promote formation of the E state. Thus, in experiments at either 7 or 40 mM Mg^{2+}, the RNA can be forced to be predominantly in the 2° or core state, respectively.

CBP2 is an RNA tertiary structure binding protein that binds preferentially to the folded RNA rather than to isolated elements of the secondary structure. Upon formation of a complex with CBP2, the RNA is in the reactive E state. Thus, whereas the RNA component contains the active site for catalysis of splicing (*3–5*), the protein enhances the rate of splicing 1000 times by holding the RNA in its active conformation. CBP2 binds at a complex site on one face of the folded RNA (Fig. 1B).

That CBP2 recognizes the tertiary structure of the intron presents a mechanistic dilemma. In most encounters between the

Department of Chemistry and Biochemistry, Howard Hughes Medical Institute, University of Colorado, Boulder, CO 80309–0215, USA.

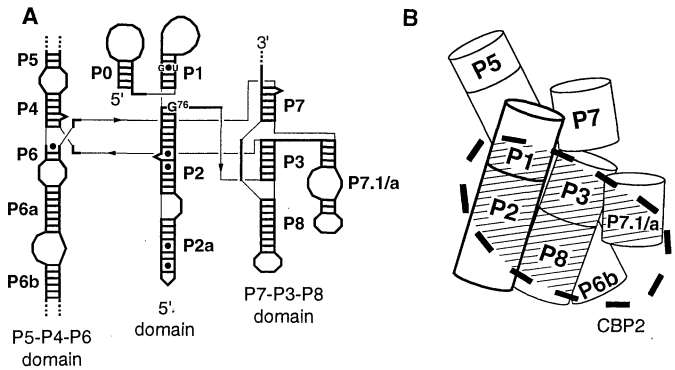

Fig. 1. Domain structure and CBP2 interaction site of bI5 RNA. (**A**) The secondary structure and connections between secondary structure elements are shown as heavy and light lines, respectively. The G·U base pair at the 5′ splice site is shown explicitly. For simplicity, some peripheral structures are omitted (dashed lines). The RNA precursor used in these experiments spans 458 nt including 5′ and 3′ exons 35 and 55 nt in length, respectively (*4*). (**B**) Schematic of bI5 RNA tertiary structure (*25*). Helices shown in A are represented as cylinders, except P0 is omitted. The CBP2 contact site on the RNA as inferred from hydroxyl radical footprinting (*3*) is shown by cross-hatching.

RNA and the splicing factor, the RNA will be in the 2° state, in which there is little tertiary folding. The question then arises, by what kinetic pathway do the intron RNA and CBP2 form an active RNP?

Using a nitrocellulose filter binding assay we determined the rate of association of bI5 RNA and CBP2 at 7 mM Mg^{2+} (*6*, *7*). As the CBP2 concentration was increased, a larger fraction of the input RNA was bound as expected (Fig. 2A). For a bimolecular association reaction, the pseudo–first-order rate constant for complex formation is expected to increase linearly with increasing concentration, as has been observed for protein association with simple RNA structures (*8*). In contrast, the observed rate constant for complex formation (0.3 min^{-1}) was independent of CBP2 concentration over a wide range (0.2 to 16 nM).

The rate of splicing for the CBP2-RNA complex is 1.2 min^{-1} (*4*), significantly faster than the observed rate of complex formation. Thus, the rate constant for complex formation could be independently determined in a splicing assay in which reaction was initiated by simultaneous addition of the splicing substrate, guanosine 5′ monophosphate (pG), and CBP2 (*9*). This assay gives additional information regarding CBP2-RNA assembly, because only complexes productive for splicing are scored. As expected, the fraction of precursor that reacted increased with increasing CBP2 concentration (Fig. 2B). However, the observed rate constant for splicing was constant at 0.3 min^{-1}.

Thus, the intrinsically bimolecular process of RNA-protein complexation exhibits a first-order rate constant. This implies that some unimolecular step is rate-limiting for RNP formation (*10*).

At 7 mM Mg^{2+}, splicing reactions initiated by addition of pG to the pre-formed CBP2-RNA complex were significantly faster than reactions initiated by addition of CBP2 and pG to free RNA (Fig. 3A, left). These data suggest that CBP2 must wait for the RNA to fold before binding. Two candidate unimolecular RNA folding steps are the transitions 2°→core and core→E (Eq. 1). If folding of the catalytic core is rate limiting for CBP2 binding at 7 mM Mg^{2+}, then at 40 mM Mg^{2+} (where the core is folded) free bI5 RNA + CBP2 should have the same splicing rate as the pre-formed RNA-CBP2 complex. This is exactly our observation (Fig. 3A, right). Binding experiments confirmed this result. At 7 mM Mg^{2+} with saturating concentrations of CBP2, a small burst of complex formation was followed by a large slow phase (~0.3 min^{-1}) (Fig. 3B). At higher Mg^{2+} concentrations the burst was much larger, followed by a slow phase again at ~0.3 min^{-1} (Fig. 3B). This is the behavior expected for binding limited by a slow conformational change (*11*): The burst reflects the rapid capture of RNA (in the core state) competent to bind protein.

Because the core is essentially folded at 40 mM Mg^{2+} (*3*), the unimolecular 2°→core transition can no longer be rate limiting for complex formation. In contrast to the concentration-independent association at 7 mM Mg^{2+}, at 40 mM Mg^{2+} the rate constant for complex formation was proportional to concentration over the range tested (0.03 to 0.2 nM CBP2) (*12*). The second-order rate constant for this reaction (3.5 ± 0.4) × 10^9 $M^{-1}min^{-1}$, is that expected for diffusion-controlled association for molecules of the size of bI5 RNA and CBP2 (*13*).

The 5′ domain makes no net contribution to binding of CBP2 to the core state. At 7 mM Mg^{2+}, the association rate of CBP2 and Δ5′ domain RNA, a mutant which begins at position G^{76} (Fig. 1A), was 0.27 ± 0.09 min^{-1} (*12*), the same within error as for the intact intron. The association rate constant was independent of CBP2 concentration over the range 3 to 24

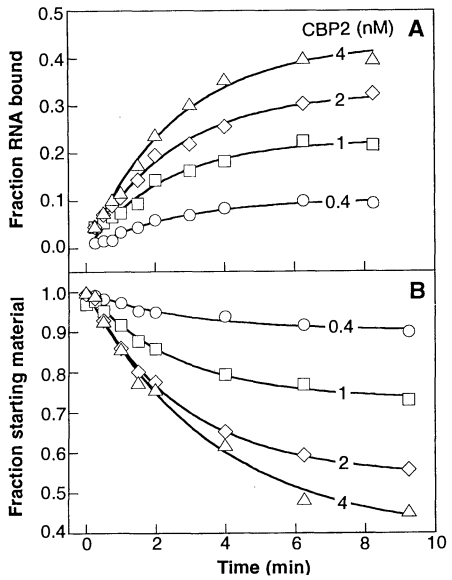

Fig. 2. Rate constant for complex formation is slow and independent of CBP2 concentration. Association rate constants were determined by two independent methods, filter binding (**A**) and splicing (**B**). CBP2 concentrations (in nM) are given for each curve. Lines represent best fits to an equation describing a first-order exponential and yield identical rate constants, 0.32 ± 0.07 min^{-1}.

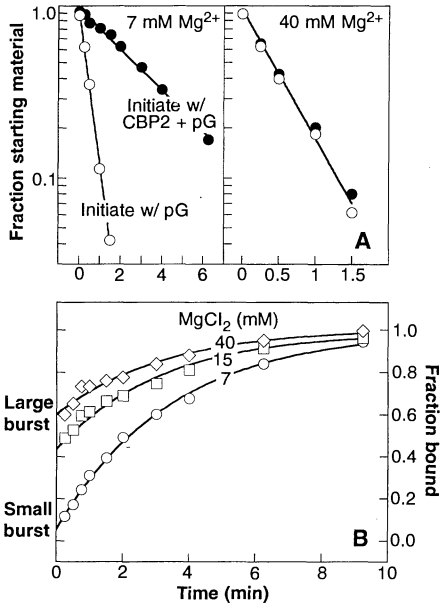

Fig. 3. Identification of the rate-limiting unimolecular step. (**A**) Order of addition experiments. Splicing reactions were initiated either by addition of pG to a pre-formed CBP2-RNA complex (open symbols) or by addition of pG and CBP2 to free bI5 RNA (solid symbols). The experiments shown in the left and right panels differ only in the concentration of Mg^{2+} in the reaction. (**B**) Burst experiments. Filter-binding reactions were performed at the indicated Mg^{2+} concentration (in mM). The burst reflects rapid binding to the core state. Points have been normalized to the fraction bound seen at long time points.

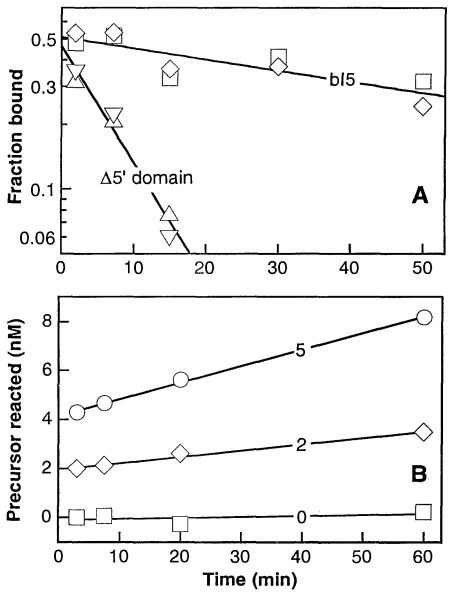

Fig. 4. Dissociation rate constants for the bI5 RNA– and Δ5′ domain–CBP2 complexes. (**A**) Rate constants were determined at 7 mM $MgCl_2$ by filter binding after trapping CBP2 binding by addition of heparin. For each complex two independent experiments were performed with different heparin concentrations of 100 (□, △) and 20 (◇, ▽) μg/ml. (**B**) Dissociation rate constant for the CBP2-bI5 RNA complex determined in a multiple turnover splicing reaction. The bI5 RNA was 100 nM; CBP2 (nM) is given for each experiment. The slope of the line divided by the protein concentration yields the dissociation rate constant, k_{dissoc} = 0.012 min^{-1}. Reactions have been corrected for 70% endpoints (*4*).

nM. However, the dissociation rate constant (at 7 mM Mg^{2+}) for the complex of CBP2 with the Δ5′ domain mutant was 13 times faster than that for the complex with intact bI5 RNA (Fig. 4A) (*14*). Because deletion of the 5′ domain increases the dissociation rate and 5′ domain association is unfavorable in the absence of CBP2 (*3*), we infer that the 5′ domain interacts with the splicing factor only after formation of the core-CBP2 complex.

We also determined the dissociation rate of the CBP2-bI5 RNA complex by an independent method in which a multiple turnover splicing assay was used (Fig. 4B). Because complex dissociation is slower than any other step in the splicing pathway, this step must be rate-limiting when RNA is in excess over protein. Under such RNA-excess conditions, splicing occurred with an initial burst, approximately stoichiometric with protein concentration (representing the first turnover), followed by a slow phase (rate-limited by complex dissociation). The dissociation rate constant (0.012 min^{-1}) was similar to that observed by direct binding measurements (0.009 min^{-1}) (Fig. 4A).

Thus, the assembly pathway for the simple RNP composed of the CBP2 protein and bI5 RNA (Fig. 5) starts with the RNA intron in a state in which the secondary structure is formed but tertiary folding is largely absent (state 2°). CBP2 does not bind stably with this state of the RNA. In a slow unimolecular conversion, the P5-P4-P6 and P7-P3-P8 domains specifically associate with each other and with other peripheral domains to form the catalytic core. The equilibrium for the 2° to core transition lies far in the direction of the 2° state in the absence of CBP2 (*3*). CBP2 then binds to the core state to capture the transiently formed tertiary structure at a rate comparable to the diffusion-controlled limit. Binding to the core state is very tight (K_d = 30 to 50 pM) (*15*). Finally, the 5′ domain associates with the CBP2-bound catalytic core in a second unimolecular step to form the active RNP enzyme, $E^{(CBP2)}$. Association of the 5′ domain realizes new stabilizing interactions to yield an RNA-protein complex whose half-life is greater than 1 hour.

Our kinetic mechanism for assembly of the bI5 intron–CBP2 RNP reveals several principles relevant to complex RNPs like the ribosome, the spliceosome, and telomerase.

1) CBP2 does not appear to increase the rate constant for any step in the forward direction. Rather, the protein captures otherwise transiently formed elements of the tertiary structure. In essence, bI5 RNA controls the assembly of its own RNP. Protein capture of a specific RNA structure has also been observed for binding of the Rom protein to an RNA loop-loop interaction (*16*).

2) Although the overall rate of assembly is slow, assembly is effectively irreversible: for every intermediate the forward rate is significantly faster than the reverse rate under conditions of saturating protein (Fig. 5).

3) Acquisition of RNA tertiary structure, as exemplified by the 2°→core transition (Fig. 5) and by a study of Mg^{2+}-induced folding of the *Tetrahymena* group I intron (*17*), occurs on a time scale of minutes. These rates of assembly of the group I intron catalytic core are much slower than observed for acquisition of tertiary structure in tRNA (*18*) or for docking of the P1 helix in the *Tetrahymena* intron (*19*), which occur on a millisecond time scale.

4) Controlled disassembly of RNPs that stabilize RNA tertiary structure is likely to be a general problem for the cell, as follows. In order to overcome the unfavorable equilibrium between the 2° and core states, CBP2 must bind to the core state very tightly (*15*). Tight binding often requires a slow dissociation rate, as has also been observed for the RNase P (ribonuclease P) holoenzyme and for a complex between the CYT18 splicing factor and the large subunit pre-ribosomal RNA (half-lives are 2 and >16 hours, respectively) (*20*, *21*). It is possible to achieve tight binding by increasing the association rate; however, CBP2 already binds at a rate near the diffusion-controlled limit. Under conditions where the protein acts in multiple turnover, dissociation of the CBP2–bI5 RNA and CYT18–intron RNA complexes is so slow as to eliminate rate enhancements achieved by protein facilitation. Thus, dissociation of these RNPs may be facilitated by other factors in vivo.

CBP2–bI5 RNA assembly shares mechanistic features with steps of assembly of the *Escherichia coli* small (30S) ribosomal subunit. In the absence of protein, the ribosomal RNA exhibits little tertiary structure (*22*). The RNA undergoes large conformational changes during assembly. Protein binding creates new RNA structures competent to form higher order architectures (*23*). The rate-limiting step for in vitro assembly corresponds to a unimolecular conformational change (*24*).

In sum, assembly of the CBP2-intron RNP involves a rate-limiting unimolecular RNA conformational change and rapid capture of transient tertiary structures by protein binding. Principles derived from this assembly mechanism are likely to be applicable to complex RNP assembly.

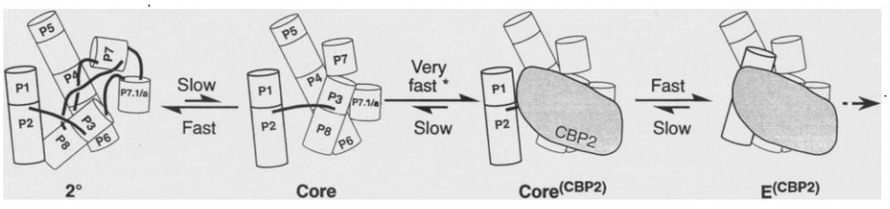

Fig. 5. Pathway of bI5 RNA–CBP2 RNP assembly at physiological Mg^{2+} concentration. All rates have been determined or estimated explicitly (*26*) and correspond to the following values: slow, 0.1 to 0.4 min^{-1}; fast, 3 to 6 min^{-1}; very fast, 14 min^{-1}. The asterisk indicates that this transition is characterized by a second-order rate constant; the rate assumes that the concentration of CBP2 = 5 × K_d = 4 nM. The dashed line following $E^{(CBP2)}$ indicates that this active RNP reacts to give splicing products.

REFERENCES AND NOTES

1. R. F. Gesteland and J. F. Atkins, Eds. *The RNA World* (Cold Spring Harbor Laboratory Press, Cold Spring Harbor, NY 1993).
2. CBP2, cytochrome b pre-mRNA processing factor 2; P. McGraw and A. Tzagoloff, *J. Biol. Chem.* **258**, 9459 (1983); A. Gampel, M. Nishikimi, A. Tzagoloff, *Mol. Cell Biol.* **9**, 5424 (1989).
3. K. M. Weeks and T. R. Cech, *Cell* **82**, 221 (1995).
4. ———, *Biochemistry* **34**, 7728 (1995).
5. A. Gampel and A. Tzagoloff, *Mol. Cell. Biol.* **7**, 2545 (1987); S. Partono and A. S. Lewin, *ibid.* **8**, 2562 (1988); A. Gampel and T. R. Cech, *Genes Dev.* **5**, 1870 (1991).
6. All reactions were performed at 35°C in 52 mM Hepes (pH 7.6), 50 mM KCl, 20 mM NaCl, either 7, 15, or 40 mM $MgCl_2$ 0.2 mM dithiothreitol (DTT), BSA at 100 μg/ml and 4% glycerol. Recombinant CBP2 protein and renatured RNAs were generated as described (*4*). All experiments were performed with ^{32}P RNA and quantified with a PhosphorImager (Molecular Dynamics).
7. Association reactions were initiated by adding RNA to a small volume containing CBP2. RNA concentrations were at least 10 times lower than the protein concentration. Reactions were quenched with heparin (final concentration, 20 to 100 μg/ml), and the fraction of RNA bound was determined by filter binding (*4*). Nonspecific binding was determined by the addition of the heparin before protein. Rates were independent of heparin concentration; however, filter binding retention efficiencies decreased with increasing heparin concentration. Association rate constants (k) were obtained from a best fit to the equation, fraction bound = $B + A(1 - e^{-kt})$, where B is the size of the burst, if any, and $A + B$ gives the endpoint.
8. A. Pingoud *et al.*, *FEBS Lett.* **30**, 1 (1973); J. Carey and O. C. Uhlenbeck, *Biochemistry* **2**, 2610 (1983); X. Gu and D. V. Santi, *ibid.* **31**, 10295 (1992); K. S. Long and D. M. Crothers, *ibid.* **34**, 8885 (1995).
9. Splicing assays were performed as described (*4*). To measure the CBP2 association rate, CBP2 and pG were added simultaneously to trace concentrations of renatured RNA. For experiments designed to measure the rate of conversion of the folded ribozyme, CBP2 was incubated with RNA for 1 hour to ensure complete binding prior to initiating splicing by addition of pG (final concentration 2 mM).
10. If the CBP2 concentration is low enough, some step involving the protein will become rate-limiting. However, this concentration must be much smaller than 0.2 nM, the lowest concentration at which we determined the association rate. At such concentrations the fraction of RNA found in a complex with CBP2 would be small.
11. For example, A. R. Fersht and Y. Requena, *J. Mol. Biol.* **60**, 279 (1971).
12. K. M. Weeks and T. R. Cech, Unpublished data.
13. R. A. Alberty and G. G. Hammes, *J. Phys. Chem.* **62**, 154 (1957); A. Fersht, *Enzyme Structure and Mecha-*

nism (Freeman, New York, ed. 2, 1985), pp. 150-152; P. H. von Hippel and O. G. Berg, *J. Biol. Chem.* **264**, 675 (1989).
14. Dissociation rates were determined by incubating renatured RNA and CBP2 for 1 hour to ensure complete binding and subsequently trapping any protein that dissociated by addition of heparin to a final concentration of 20 to 500 μg/ml. Fraction RNA bound was analyzed by filter binding (*4*). Dissociation rates were independent of heparin concentration. Endpoints were obtained from reactions in which the heparin was added before CBP2.
15. We estimate the equilibrium dissociation constant for protein binding to the core state either (i) by correcting the observed K_d for the fraction of properly folded RNA or (ii) from the elemental rate constants for the core⇄core^{CBP2} interconversion: (i) The observed K_d is 0.8 nM (*4*), whereas the equilibrium constant for formation of the core state is 0.07 (*3*). Thus, the K_d for binding to the core is equal to (0.8 nM) × [0.07/(1+0.07)] = 50 pM. (ii) The reverse and forward rates for formation of the core^{CBP2} state are taken as the rate of dissociation of the CBP2-Δ5′ domain RNA complex (Fig. 4) and the rate constant for formation of core^{CBP2} at 40 mM Mg^{2+}, respectively; K_d = (0.12 min^{-1})/(3.5 × 10^9 M^{-1} min^{-1}) = 30 pM.
16. Y. Eguchi and J.-I. Tomizawa, *Cell* **60**, 199 (1990).
17. P. P. Zarrinkar and J. R. Williamson, *Science* **265**, 918 (1994).
18. P. E. Cole and D. M. Crothers, *Biochemistry* **11**, 4368 (1972); D. M. Crothers, P. E. Cole, C. W. Hilbers, R. G. Schulman, *J. Mol. Biol.* **87**, 63 (1974).
19. P. C. Bevilacqua, R. Kierzek, K. A. Johnson, D. H. Turner, *Science* **258**, 1355 (1992); D. Herschlag, *Biochemistry* **31**, 1386 (1992); Y. Li, P. C. Bevilacqua, D. Mathews, D. H. Turner, *ibid.* **34**, 14394 (1995).
20. S. J. Talbot and S. Altman, *ibid.* **33**, 1406 (1994).
21. CYT18, mitochrondrial tyrosyl tRNA synthetase which facilitates splicing of group I introns in *Neurospora crassa*; R. J. Saldanha, S. S. Patel, R. Surendran, J. C. Lee, A. M. Lambowitz [*ibid.* **34**, 1275 (1995)] observed rapid formation of an initial CYT18 pre–ribosomal RNA complex characterized by a second-order rate constant, in contrast to our observations with bI5 RNA. These data emphasize that there exist alternate pathways for simple RNP assembly.
22. T. Powers and H. F. Noller, *RNA* **1**, 194 (1995); V. Mandiyan, S. J. Tumminia, J. S. Wall, J. F. Hainfield, M. Boublik, *J. Mol. Biol.* **210**, 323 (1989).
23. M. Nomura, S. Mizushima, M. Ozaki, P. Traub, C. V. Lowry, *Cold Spring Harbor Symp. Quant. Biol.* **34**, 49 (1969); W. A. Held, B. Ballou, S. Mizushima, M. Nomura, *J. Biol. Chem.* **249**, 3103 (1974); T. Powers, G. Daubresse, H. F. Noller, *J. Mol. Biol.* **232**, 362 (1993).
24. W. A. Held and M. Nomura, *Biochemistry* **12**, 3273 (1973). Assembly of the large subunit of the ribosome involves two rate-limiting unimolecular transitions [G. Sieber and K. H. Nierhaus, *ibid.* **17**, 3505 (1978)].
25. F. Michel and E. Westhof, *J. Mol. Biol.* **216**, 585 (1990); L. Jaeger, E. Westhof, F. Michel, *ibid.* **221**, 1153 (1991).
26. (i) $k(2° \rightarrow \text{core}) = 0.3\ min^{-1}$ (Fig. 2). The rate constant for the reverse reaction for this step, $k(\text{core} \rightarrow 2°)$, was calculated from the rate constant for the forward reaction divided by the equilibrium constant (*3*), (0.3 min^{-1})/(0.07) = 4 min^{-1}. (ii) $k(\text{core} \rightarrow \text{core}^{CBP2}) = 3.5 \times 10^9\ M^{-1}\ min^{-1}$ was determined at 40 mM $MgCl_2$ and provides an estimate for the value at 7 mM $MgCl_2$. The rate constant for the reverse reaction, $k(\text{core}^{CBP2} \rightarrow \text{core})$, is taken to equal the dissociation rate for the Δ5′ domain–CBP2 complex (0.12 min^{-1}; Fig. 4). (iii) The equilibrium constant for the core^{CBP2}⇄E^{CBP2} transition is given by the ratio of dissociation rate constants for the bI5- and Δ5′-domain–CBP2 complexes [W. W. Cleland, *Biochemistry* **14**, 3220 (1974); data from Fig. 4], (0.12 min^{-1}/0.009 min^{-1}) = 13. $k(\text{core}^{CBP2} \rightarrow E^{CBP2})$ must be faster than 2 min^{-1}, the rate of splicing of the E^{CBP2} state (*4*).
27. We thank P. Bevilacqua for discussion. Supported by a fellowship from the Jane Coffin Childs Memorial Fund for Medical Research (K.M.W.) and by the Howard Hughes Medical Institute (T.R.C.).

24 July 1995; accepted 29 December 1995

C3d of Complement as a Molecular Adjuvant: Bridging Innate and Acquired Immunity

Paul W. Dempsey, Michael E. D. Allison, Srinivas Akkaraju, Christopher C. Goodnow, Douglas T. Fearon*

An optimal immune response should differentiate between harmful and innocuous antigens. Primitive systems of innate immunity, such as the complement system, may play a role in this distinction. When activated, the C3 component of complement attaches to potential antigens on microorganisms. To determine whether this alters acquired immune recognition, mice were immunized with a recombinant model antigen, hen egg lysozyme (HEL), fused to murine C3d. HEL bearing two and three copies of C3d was 1000- and 10,000-fold more immunogenic, respectively, than HEL alone. Thus, C3d is a molecular adjuvant of innate immunity that profoundly influences an acquired immune response.

The decision of the acquired immune system to respond to an antigen may be based not only on what is non-self, but also on what is infectious and of potential danger to the host (*1*). How the immune system makes this latter determination is not clear because the antigen receptors that are distributed among different lymphocyte clones generally cannot distinguish between noxious and innocuous antigens.

Systems of innate resistance to infection evolved before acquired immunity and are triggered by certain biochemical characteristics that are shared by microorganisms but not by higher forms of life. Complement is a plasma protein system of innate immunity that is activated by microorganisms in the absence of antibody (*2*). One consequence of activation is the covalent attachment of fragments of the third complement protein, C3, to the activator, and two of these fragments, C3dg and C3d, bind to CR2 (CD21) on B lymphocytes. CD21 may have B cell–stimulating functions because it associates with CD19, a B cell membrane protein that amplifies B cell activation (*3*) and is required for normal T cell–dependent, B cell responses (*4*). In support of this, depleting mice of C3 or blocking the binding of ligand to CD21 raises by approximately 10-fold the threshold dose of antigen required to elicit antibody (*5*, *6*). Therefore, the complement system may be an innate immune system that provides information to the acquired immune system in an attempt to classify antigens according to their potential hazard.

To determine whether the immunity-enhancing function of complement is mediated solely by the attachment of C3d to antigen and, if so, the magnitude of this effect of C3d, we prepared recombinant model antigens of hen egg lysozyme (HEL)

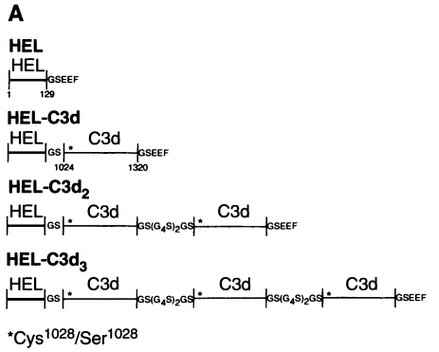

Fig. 1. Recombinant HEL and HEL-C3d fusion proteins. (**A**) Recombinant proteins comprising amino acids 1 to 129 of HEL alone and fused to one, two, or three copies of amino acids 1024 to 1320 of the C3d region of murine C3 were prepared (*7*). Amino acids in addition to those present in the native proteins are Gly (G), Ser (S), Glu (E), Phe (F), and Ser that was substituted for Cys (C) at position 1028 of C3 to avoid the presence of a free sulfhydryl in the recombinant proteins. (**B**) The recombinant proteins were purified from culture supernatants of transfected cells and assessed by SDS–polyacrylamide gel electrophoresis and Coomassie blue staining. Size markers are on the left in kilodaltons.

P. W. Dempsey, M. E. D. Allison, D. T. Fearon, Wellcome Trust Immunology Unit, Department of Medicine, University of Cambridge School of Medicine, Cambridge CB2 2SP, UK.
S. Akkaraju, Program in Immunology, Stanford University School of Medicine, Stanford, CA 94305–5428, USA.
C. C. Goodnow, Howard Hughes Medical Institute, Department of Microbiology and Immunology, Stanford University School of Medicine, Stanford, CA 94305–5428, USA.
*To whom correspondence should be addressed.